Journal of Medicinal Chemistry

ARTICLE

pubs.acs.org/jmc

Structure−Activity Relationships of Phosphoinositide 3-Kinase (PI3K)/Mammalian Target of Rapamycin (mTOR) Dual Inhibitors: Investigations of Various 6,5-Heterocycles to Improve Metabolic Stability

Markian M. Stec,*[,†] Kristin L. Andrews,[∥] Shon K. Booker,[†] Sean Caenepeel,[‡] Daniel J. Freeman,[‡] Jian Jiang,[§] Hongyu Liao,[†] John McCarter,[⊥] Erin L. Mullady,[⊥] Tisha San Miguel,[⊥] Raju Subramanian,[§] Nuria Tamayo,[†] Ling Wang,[‡] Kevin Yang,[†] Leeanne P. Zalameda,[⊥] Nancy Zhang,[‡] Paul E. Hughes,[‡] and Mark H. Norman[†]

[†]Department of Medicinal Chemistry, [‡]Department of Oncology, [§]Department of Pharmacokinetics and Drug Metabolism, [∥]Department of Molecular Structure, [⊥]Department of High-Throughput Screening/Molecular Pharmacology, Amgen Inc., One Amgen Center Drive, Thousand Oaks, California 91320-1799, United States, and 360 Binney Street, Cambridge, Massachusetts 02142, United States

Supporting Information

ABSTRACT: *N*-(6-(6-Chloro-5-(4-fluorophenylsulfonamido)pyridin-3-yl)benzo[*d*]thiazol-2-yl)acetamide (**1**) is a potent and efficacious inhibitor of PI3Kα and mTOR in vitro and in vivo. However, in hepatocyte and in vivo metabolism studies, **1** was found to undergo deacetylation on the 2-amino substituent of the benzothiazole. As an approach to reduce or eliminate this metabolic deacetylation, a variety of 6,5-heterocyclic analogues were examined as an alternative to the benzothiazole ring. Imidazopyridazine **10** was found to have similar in vitro potency and in vivo efficacy relative to **1**, while only minimal amounts of the corresponding deacetylated metabolite of **10** were observed in hepatocytes.

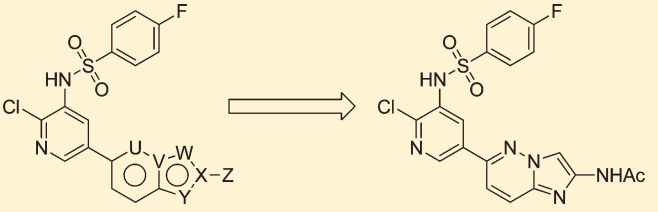

INTRODUCTION

Phosphoinositide 3-kinases (PI3Ks) phosphorylate the 3-hydroxyl group of the inositol ring of phosphoinositides. PI3Ks are grouped into three classes, with PI3Kα being in the class IA subgroup and consisting of a heterodimeric p85 regulatory subunit and a p110 catalytic subunit. Other class IA PI3Ks include PI3Kβ and PI3Kδ, while PI3Kγ falls in the class IB subgroup. Activation of class I PI3Ks results in the initiation of a signal transduction cascade leading to the phosphorylation of the serine-threonine kinase Akt (also known as PKB) that in turn promotes cell growth, survival, and cell cycle progression. Another relevant class of kinases is the PI3K-related kinases (PIKKs) that are protein kinases with a catalytic domain homologous to PI3Ks. One particularly important member of the PIKK family is mTOR (mammalian target of rapamycin) which plays an integral key role in regulating class I PI3K activation and signaling.[1−3]

Many human cancers have activated PI3K signaling, often as a result of gain-of-function mutations in PI3Kα[4,5] or loss-of-function mutations in PTEN[1] (a phosphatase that performs the reverse phosphorylation event performed by class I PI3Ks). These genetic alterations strongly link constitutive PI3K signaling to tumorigenesis and have stimulated an interest in targeting PI3Kα, and other kinases in the PI3K/Akt pathway, for the treatment of cancer. There are currently at least 15 PI3K inhibitors in clinical development.[6−8] These clinical candidates have varying selectivity profiles toward different class I PI3K isoforms and mTOR and the optimal selectivity profile for efficacy against specific tumor types remains to be determined.[6−13]

In our efforts to identify novel inhibitors of this pathway, we identified benzothiazole **1**, which was found to be a potent inhibitor of PI3Kα in vitro (K_i = 1.2 nM in the enzymatic assay, IC_{50} = 6.3 nM in the U87 MG cellular assay) (Figure 1).[14,15] This compound was also a potent inhibitor of the other class I PI3Ks β, γ, and δ as well as mTOR and was selective against many protein kinases. Furthermore, compound **1** showed efficacy in a variety of tumor xenograft models in mice (e.g., ED_{50} = 0.26 mg/kg, once daily (QD), U87 MG tumor xenograft model).

Compound **1** was stable in plasma and exhibited low clearance (<26 μL/min/mg) in liver microsomes (mouse, rat, dog, monkey, and human[16]) and low (0.2−1.4% of liver blood flow) in vivo clearance in mouse, rat, and dog. However, metabolite profiling in hepatocytes showed that **1** underwent deacetylation to give compound **2**, which itself was a potent inhibitor of PI3Kα (Figure 1). Differential formation of **2** was observed across species, with dog and human forming more of **2** than rat and monkey. Analysis of plasma in rat and dog, post oral dosing,

Received: April 13, 2011
Published: June 29, 2011

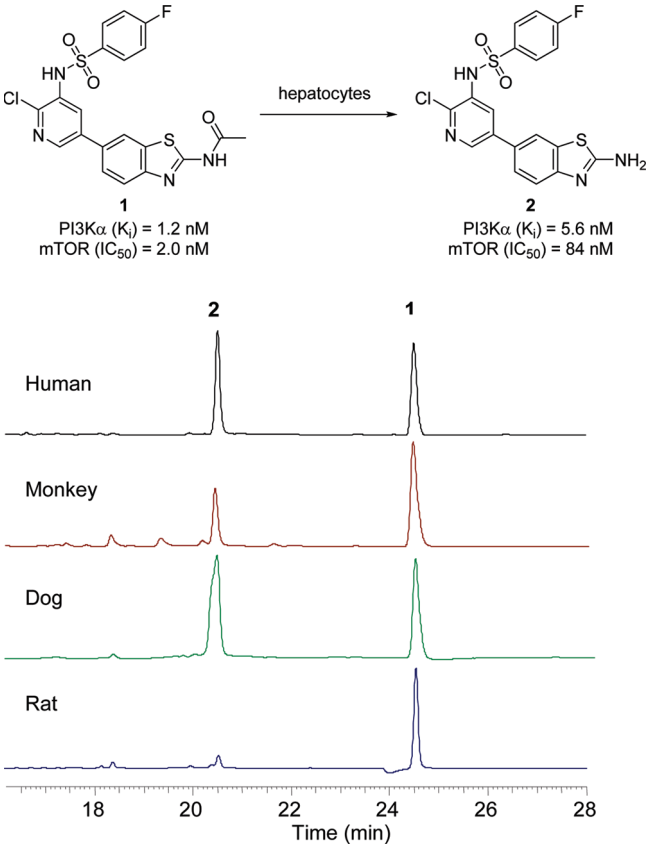

Figure 1. Deacetylation of **1** in hepatocytes. Reverse-phase HPLC UV (308 nm) chromatographs of supernatant liquid, post centrifugation, obtained from incubation of hepatocytes with **1** for 2 h at 37 °C.

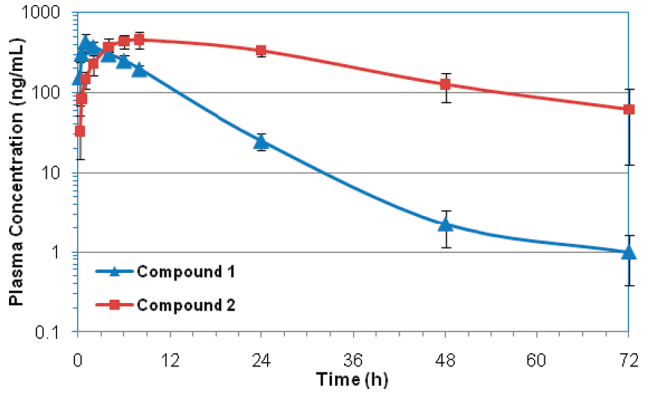

Figure 2. In vivo plasma levels of **1** and **2** in dog post administration of a 0.3 mg/kg oral dose of compound **1**. Each time-point is a mean plasma concentration from 3 dogs; vehicle was 20% captisol, 2% HPMC, and 1% Tween 80.

revealed the presence of both **1** and **2** across the pharmacokinetic profile. For example, in dog, deacetylated metabolite **2** levels were equal to or higher than that of compound **1** at all time points greater than 2 h (Figure 2). In dog, the plasma AUC ratio of compound **2** versus compound **1** was 4.6, while in rat that ratio was 0.6−0.8 (data not shown). Across species, there was a qualitative relationship between the amount of **2** found from in vitro incubation of **1** and the in vivo plasma level of **2** observed upon oral administration of **1**. Therefore, in humans, the hepatocyte data suggested that administration of **1** would also lead to a significant concentration of active metabolite **2** in plasma. Because formation of this active metabolite would complicate drug development efforts of **1**, an alternative compound was sought.

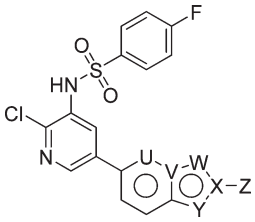

Figure 3. Alternative 6,5-heterocyclic ring systems as derivatives of compound **1**.

To avoid this metabolic deacetylation issue, we took one approach where the benzothiazole moiety was replaced with various 6,6-bicyclic ring systems that did not contain the *N*-acetyl group.[17] This work led to the identification of a potent series of quinoline and quinoxaline PI3K inhibitors with good pharmacokinetic properties. An alternative approach, which is described in this paper, was to replace the benzothiazole ring system with other 6,5-heterocyclic ring systems (Figure 3) that could either reduce the rate of deacetylation or retain sufficient activity in the absence of the *N*-acetyl group. Toward this end, we prepared and evaluated several 6,5-heterocyclic analogues of **1** where U−Y were replaced with various combinations of heteroatoms to give imidazopyridazines, imidazopyridines, benzimidazoles, benzoxazoles, triazolopyridines, and benzoisothiazoles. In addition, we prepared a set of analogues with small variations of the Z substituent (Z = NHAc, NH_2, H) to explore the effect of altering the nature of the hydrogen bond donor in this area of the molecule.

CHEMISTRY

The majority of the 6,5-heterocyclic analogues of **1** were prepared as outlined in Scheme 1. The synthesis began with 5-bromo-2-chloropyridin-3-amine (**3**), which was treated with 4-fluorobenzene-1-sulfonyl chloride (**4**) under basic conditions to afford sulfonamide **5**.[18] Compound **5** was converted to pinacol boronic ester **7** under palladium-catalyzed borylation conditions utilizing bis(pinacolato)diboron (**6**).[19] Boronic ester **7** was then coupled to heterocyclic halides **8** under a variety of palladium-catalyzed cross-coupling conditions to provide analogues **9**, **10**, and **12**−**22**. Aminoimidazopyridazine **11** was obtained by basic hydrolysis of the corresponding *N*-acetyl derivative, **10**. The requisite heterocyclic halides **8** were obtained through commercial suppliers, precedented syntheses, or their syntheses are described in the Supporting Information.

The final two analogues, benzoxazole **24** and benzisothiazole **27**, were synthesized by reversing the coupling partners in the palladium-catalyzed cross-coupling reaction (Scheme 2). Aryl bromide **22** underwent palladium-catalyzed borylation,[19] followed by conversion to the trifluoroborate salt[20] to afford **23**. Subsequent coupling with bromopyridine **5** afforded benzoxazole **24**. Similarly, aryl bromide **25** was converted to boronic ester **26**, which when coupled to bromopyridine **5**, provided the final target, benzoisothiazole **27**.

dx.doi.org/10.1021/jm2004442 |*J. Med. Chem.* 2011, 54, 5174–5184

Scheme 1[a]

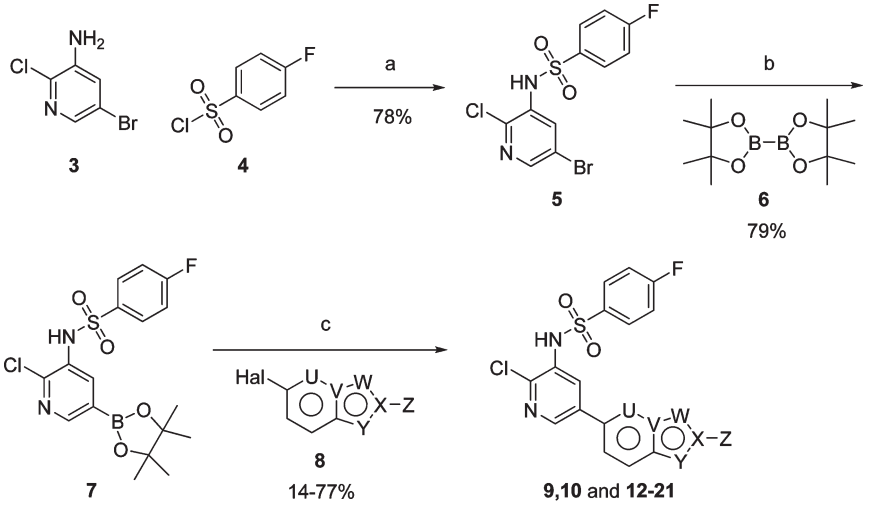

		U	V	W	X	Y	Z
	9	C	C	S	C	N	H
d 15%	**10**	N	N	C	C	N	NHAc
	11	N	N	C	C	N	NH_2
	12	N	N	C	C	N	H
	13	C	N	C	C	N	NHAc
	14	C	N	C	C	N	NH_2
	15	C	N	C	C	N	H

	U	V	W	X	Y	Z
16	C	C	N	C	N	NHAc
17	C	C	N	C	N	NH_2
18	C	C	N	C	N	H
19	C	C	O	C	N	NH_2
20	C	C	O	C	N	H
21	C	N	C	N	N	---

[a] Reagents and conditions: (a) NaHMDS, THF, 25 °C; (b) $PdCl_2$(dppf), KOAc, 1,4-dioxane, 100 °C; (c) Pd catalyst, base; (d) aq NaOH, MeOH, 100 °C.

Scheme 2[a]

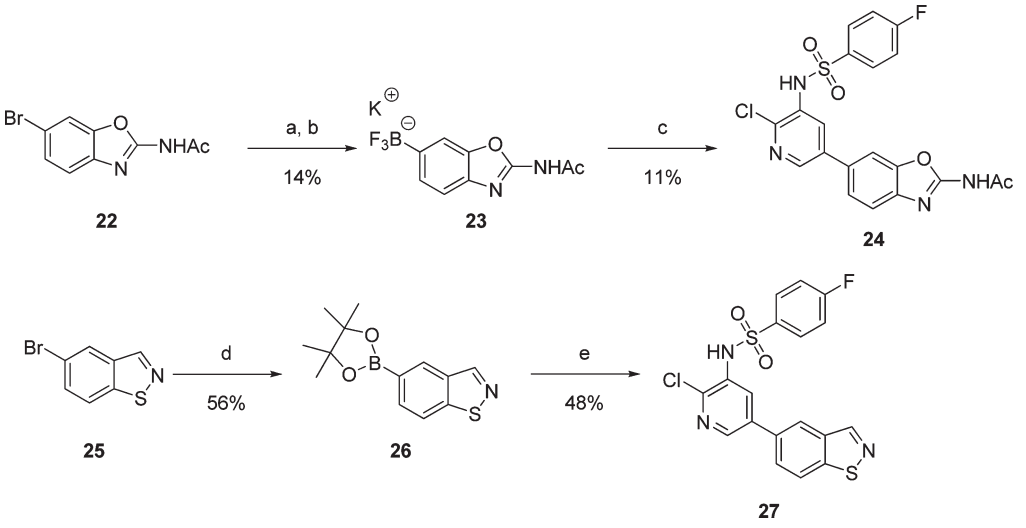

[a] Reagents and conditions: (a) **6**, $PdCl_2$(dppf), KOAc, 1,4-dioxane, 100 °C. ;(b) KHF_2, CH_3CN; (c) **5**, $PdCl_2$(dppf), Cs_2CO_3, THF, 100 °C, microwave; (d) **6**, $Pd_2(dba)_3$, PCy_3, KOAc, 1,4-dioxane, 110 °C, microwave; (e) **5**, FibreCat 1029 triphenylphosphine, aq Na_2CO_3, 1,4-dioxane, 110 °C, microwave.

RESULTS AND DISCUSSION

The various 6,5-ring system analogues of **1** were examined in two enzyme assays to determine the inhibition of PI3Kα and mTOR activity and in a cellular assay that determined Akt (Ser 473) phosphorylation in U87 MG cells.[14] The results are shown in Table 1. In general, the compounds were moderate to potent inhibitors of PI3Kα and showed comparable mTOR potencies (within an order of magnitude) with the exception of compound **21**, which was significantly less active toward mTOR. Therefore, for the purposes of the structure−activity relationship (SAR) discussion, we will focus on the PI3Kα activity. Compound **2**, the nonacetylated derivative of compound **1**, showed 5-fold lower

dx.doi.org/10.1021/jm2004442 |J. Med. Chem. 2011, 54, 5174–5184

Table 1. In Vitro Potency of PI3Kα Inhibitors[a]

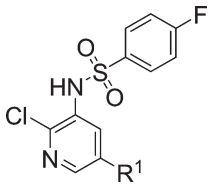

compd	R^1	R^2	PI3Kα (K_i, nM)[b]	mTOR (IC_{50}, nM)[b]	pAkt (U87 MG) (IC_{50}, nM)[b]
1	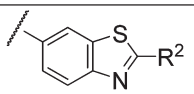	-NHAc	1.2 ± 0.9	2.0 ± 4.8	6.3 ± 6.5
2		$-NH_2$	5.6 ± 3	24 ± 8	44
9		-H	13 ± 8	33 ± 16	769 ± 300
10	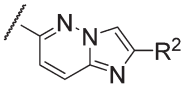	-NHAc	1.4 ± 0.7	0.4 ± 0.2	13 ± 6
11		$-NH_2$	11 ± 2	35 ± 44	415
12		-H	6.1 ± 0.9	49 ± 27	50
13	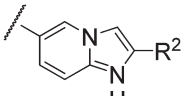	-NHAc	1.2 ± 0.5	6.6 ± 4.0	118
14		$-NH_2$	2.8 ± 0.6	20 ± 14	>12,000
15		-H	23 ± 9	229	574
16	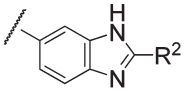	-NHAc	3.3 ± 0.6	20 ± 13	335
17		$-NH_2$	119 ± 73	430	>12,000
18		-H	68 ± 11	446 ± 88	>12,000
24	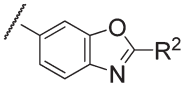	-NHAc	47 ± 4	146	1,100
19		$-NH_2$	7.2 ± 0.4	70	101
20		-H	26 ± 3	76 ± 35	>12,000
21	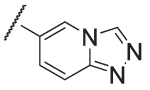	N/A	51 ± 2	>25,000	>12,000
27	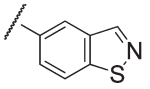	N/A	76 ± 10	292	>12,000

[a] See ref 14 for assay details. [b] The results without a SD are from a single experiment.

potency in the PI3Kα enzyme assay and a 7-fold reduction in cellular potency relative to **1**. Having no substitution on the 2-position of the benzothiazole, compound **9** showed a significant reduction in cellular activity relative to **1** and **2**.

Imidazopyridazines **10**−**12** and imidazopyridines **13**−**15** showed good to excellent PI3Kα enzyme potencies (1−23 nM); however, the majority of these analogues showed a dramatic loss in cellular potency, with the exception of compound **10** and **12**, which maintained cellular activities of 13 and 50 nM, respectively.

In the benzimidazole series (**16**−**18**), only the 2-acetamide analogue (**16**) had single-digit nanomolar potency in the PI3Kα enzyme assay. The other two benzimidazole analogues, **17** and **18**, demonstrated decreased PI3Kα enzyme activities and all three benzimidazole analogues gave poor cellular potencies (>300 nM). Benzoxazole analogues **19**, **20**, and **24** exhibited moderate to good potencies in the PI3Kα enzyme assay, but a significant loss in activity was observed in the cellular assay with values of >100 nM. Interestingly, the nonacetylated aminobenzoxazole **19** showed the greatest PI3Kα enzyme potency of the benzoxazoles; however, this did not translate to acceptable functional activity.

Triazolopyridine **21** and benzoisothiazole **27** precluded substitution at the 2-position and afforded diminished potency relative to the 2-acetamide compounds such as **1**, **10**, and **13** and supported the observation that substitution at the 2-position

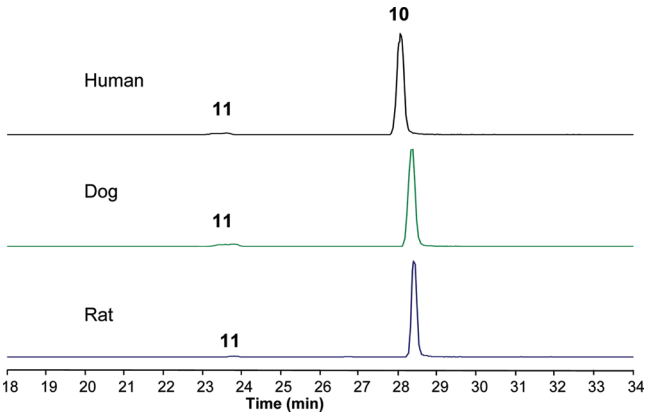

Figure 4. Deacetylation of imidazopyridazine **10** in human, dog, and rat hepatocytes. Reverse-phase HPLC extracted ion MS chromatographs of supernatant liquid, post centrifugation, obtained from incubation of hepatocytes with **10** for 2 h at 37 °C.

was preferred. However, compounds **21** and **27** had similar PI3Kα enzyme activities (within an order of magnitude) relative to compounds with Z = H, such as **9**, **12**, **15**, **18**, and **20**.

Taken together, the results outlined in Table 1 show that the acetylated compounds (R^2 = NHAc) generally showed the best potencies compared to the amino compounds ($R^2 = NH_2$) or the

dx.doi.org/10.1021/jm2004442 |J. Med. Chem. 2011, 54, 5174–5184

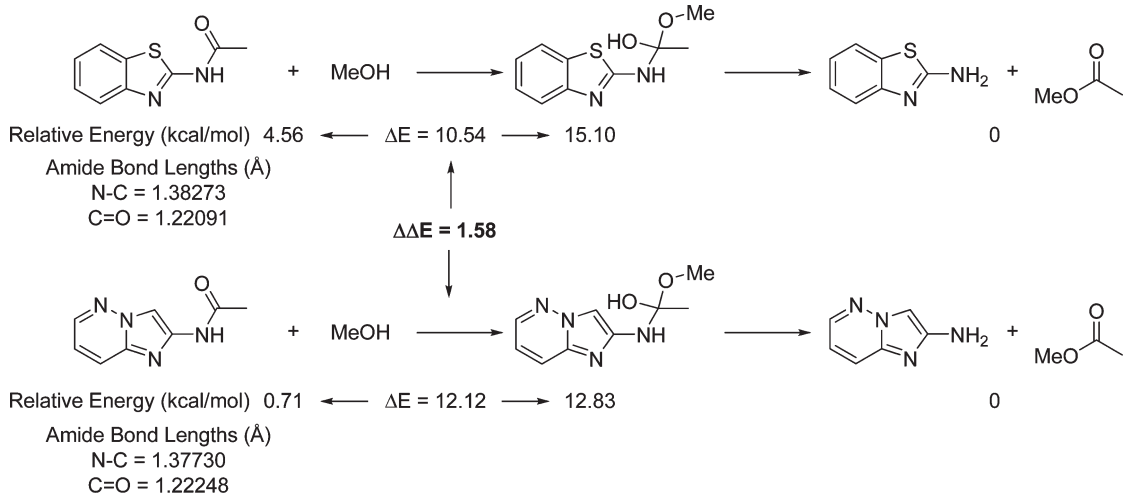

Figure 5. Comparison of calculated bond lengths and energies of formation of tetrahedral intermediates for 2-acetamidobenzothiazole and 2-acetamidoimidazopyridazine.

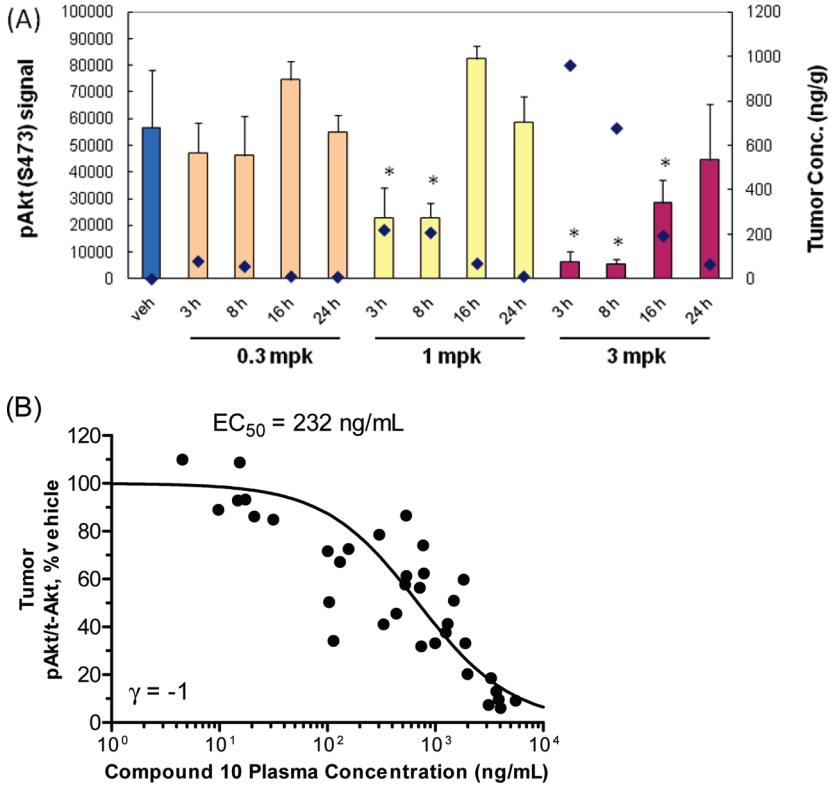

Figure 6. (A) Effect of compound **10** on Akt (Ser 473) phosphorylation in U87 MG tumors. Asterisk denotes $p < 0.01$ compared with the vehicle group. Bars represent the mean ± SD ($n = 3$). Diamonds represent mean tumor concentration. (B) Plot of plasma concentrations vs percent inhibition of Akt phosphorylation. The percent inhibition was calculated relative to vehicle from the measured ratios of phosphorylated Akt (pAkt) to total Akt (t-Akt) in U87 MG tumors in the dose−response and time course PD experiments. γ is the Hill coefficient, and the solid line represents a nonlinear regression fit from a sigmoidal dose−response model.

unsubstituted compounds (R^2 = H), with the benzoxazole series being the exception. Within the acetylated analogues, only imidazopyridazine **10** showed comparable enzyme and cellular activities to benzothiazole **1**. In addition, compound **10** showed a similar selectivity profile to **1** in that it was a potent inhibitor of mTOR (IC_{50} = 0.4 nM) and other class I PI3Ks (β, γ, and δ; K_i = 3.5, 1.9, and 0.8 nM, respectively). In a kinase selectivity screen[21] profiling activity on 402 protein and lipid kinases, compound **10** was only active on PI3Ks (percentage of control (POC) = 0−1.4%) and moderately active (POC = 10−25%) on three kinases (YSK4, ERK8, and PIK4CB). For all other kinases in the panel, compound **10** showed little or no kinase activity

dx.doi.org/10.1021/jm2004442 |J. Med. Chem. 2011, 54, 5174–5184

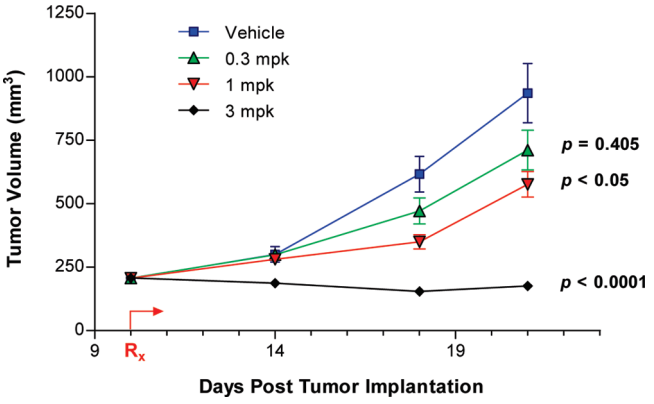

Figure 7. Daily dosing with imidazopyridazine **10** induced tumor stasis and growth delay in established U87 MG glioblastoma xenograft model. Arrow denotes the first day of dosing. Data points represent the mean ± SE (n = 10). Statistical significance was evaluated by Repeated Measures ANOVA followed by Dunnett post hoc test.

(POC = 36−100%). Kinase activity was measured as a percentage of control (POC) when treated with compound **10** at a concentration of 1 μM.[22]

To determine whether the change to an imidazopyridazine core from a benzothiazole core affected its propensity to deacetylate, compound **10** was incubated in microsomes and primary hepatocytes from different species. The hepatocyte metabolite profiles are shown in Figure 4. Only trace levels of deacetylated-**10** (compound **11**) were detected in vitro.

In attempting to rationalize the increased stability of **10** toward deacetylation, we noted that during our synthetic studies, imidazopyridazine **10** required stronger conditions for deacetylation than benzothiazole **1**. For example, after treatment with Cs_2CO_3 in MeOH, H_2O, and DMF for 3 h at 70 °C, compound **1** underwent complete deacetylation while compound **10** showed no appreciable deacetylation under the same conditions. The increased chemical stability of the 2-acetamidoimidazopyridazine toward deacetylation may be due to the relative strengths of the amide bonds. The calculated N−C amide bond length in the 2-acetamidoimidazopyridazine derivative was 1.377 Å versus 1.383 Å for the 2-acetamidobenzothiazole (Figure 5). This calculated bond length difference could be attributed to the availability of an additional tautomer delocalizing the amide bond into the benzothiazole ring that is not available in the imidazopyridazine case. In addition, quantum mechanics calculations of the neutral tetrahedral intermediates suggest that higher energy is required for the 2-acetamidoimidazopyridazine to proceed from the acetamide to a tetrahedral intermediate versus the 2-acetamidobenzothiazole ($\Delta\Delta E$ = 1.58 kcal/mol), which may also contribute to the increased hepatocyte stability of the 2-acetamidoimidazopyridazine system.[23,24]

With its excellent in vitro cellular potency and improved metabolic stability, imidazopyridazine **10** was further evaluated in pharmacokinetic and pharmacodynamic (PD) studies. In rats, intravenous dosing of compound **10** demonstrated a low clearance (0.04 L/h/kg; 1.2% of liver blood flow) and a low volume of distribution (0.27 L/kg) with an elimination half-life of 7 h. Compound **10** dosed orally in rats at 2 mg/kg showed good oral bioavailability (46%) and a high plasma exposure (AUC = 11500 ng·h/mL). The in vivo activity of compound **10** was evaluated in a mouse pharmacodynamic assay in U87 MG tumors. Tumor bearing mice were treated with a single oral dose of compound **10** at 0.3, 1, or 3 mg/kg and the tumors were harvested at 3, 8, 16, and 24 h postdose. Figure 6A illustrates Akt (Ser 473) phosphorylation (bar graph) and the observed tumor concentrations of compound **10** (blue diamonds). Plasma concentrations were also determined in this study and were found to be 1−8 times higher than tumor concentrations.[25] Treatment with compound **10** at 1 mg/kg resulted in a significant inhibition ($p < 0.01$) of Akt phosphorylation for up to 8 h with a mean tumor to plasma ratio of 0.13 at that time point. At the 3 mg/kg dose, significant inhibition of Akt phosphorylation was observed up to 16 h with a mean tumor to plasma ratio of 0.27. A plot of plasma concentration versus percent inhibition of Akt phosphorylation in the U87 MG tumors is shown in Figure 6B and a nonlinear regression analysis revealed a low plasma EC_{50} (0.5 μM, 232 ng/mL).

Given the clear pharmacodynamic effect of compound **10**, it was evaluated for its ability to inhibit tumor growth in the mouse U87 MG glioblastoma xenograft model.[14] Treatment with compound **10** at 1 mg/kg QD resulted in significant inhibition of tumor growth of 49% compared to the vehicle control group, while treatment with 3 mg/kg QD resulted in tumor stasis. The ED_{50} of compound **10** was 0.7 mg/kg (AUC at ED_{50} of 9.2 μg·h/mL) (Figure 7).[26] Compound **10** was well tolerated as judged by minimal body weight loss (<5% compared to predose weight) at the highest dose.

CONCLUSION

In conclusion, a potent and efficacious PI3Kα/mTOR inhibitor **1** was found to undergo deacetylation in human hepatocytes to form an active metabolite **2**; therefore, an alternative derivative was sought that would not have this liability. Various 6,5-heterocyclic ring systems were explored and imidazopyridazine **10** was found to have comparable in vitro potency and in vivo efficacy relative to **1** yet it was more metabolically stable and underwent minimal deacetylation upon incubation in rat, dog, and human hepatocytes.

EXPERIMENTAL METHODS

Chemistry. All reactions were conducted in a well-ventilated fume hood under N_2 using a Teflon-coated magnetic stir bar at the temperature indicated. Reactions heated by microwave utilized a CEM brand microwave utilizing 100 W of energy with Powermax (simultaneous heating while cooling technology) feature turned on. All solvents and reagents obtained from commercial sources were used without further purification. Unless otherwise indicated, removal of solvents was conducted by using a rotary evaporator, and residual solvent was removed from nonvolatile compounds using a vacuum manifold maintained at approximately 1 Torr. All yields reported are isolated yields.

^{1}H NMR spectra were obtained on a Bruker BioSpin GmbH magnetic resonance spectrometer. ^{1}H NMR spectra are reported as chemical shifts in parts-per-million (ppm) relative to an internal solvent reference. Peak multiplicity abbreviations are as follows: s (singlet), br s (broad singlet), d (doublet), dd (doublet of doublets), t (triplet), q (quartet), quin (quintet), and m (multiplet).

Analytical HPLC and mass spectroscopy were conducted using a reverse-phase Agilent 1100 Series HPLC-mass spectrometer. Purities for final compounds were measured using UV detection at 254 nm and are ≥95.0%.

***N*-(5-Bromo-2-chloropyridin-3-yl)-4-fluorobenzenesulfonamide (5).** To a 100 mL, round-bottomed flask was added 5-bromo-2-chloropyridin-3-amine (0.500 g, 2.41 mmol) and THF (10 mL).

dx.doi.org/10.1021/jm2004442 |J. Med. Chem. 2011, 54, 5174–5184

Sodium bis(trimethylsilyl)amide (1.33 g, 7.23 mmol) was added to the mixture and stirred for 10 min. 4-Fluorobenzene-1-sulfonyl chloride (1.41 g, 7.23 mmol) was then added, and the solution was stirred at room temperature overnight. The reaction mixture was diluted with satd $NaHCO_3$ and extracted with DCM (4 × 30 mL). The combined extracts were dried (Na_2SO_4), filtered, and concentrated in vacuo. Purification by silica gel chromatography (1−30% EtOAc/DCM) afforded **5** as a tan solid (0.690 g, 78% yield). MS (ESI positive ion) m/z: 366.9 (M + 1). ^{1}H NMR (400 MHz, DMSO-d_6): δ ppm 7.35−7.48 (m, 2H), 7.79−7.86 (m, 2H), 7.94 (d, J = 2.5 Hz, 1H), 8.43 (d, J = 2.0 Hz, 1H), 10.65 (br s, 1H).

***N*-(2-Chloro-5-(4,4,5,5-tetramethyl-1,3,2-dioxaborolan-2-yl)pyridin-3-yl)-4-fluorobenzenesulfonamide (7).** To a 100 mL, round-bottomed flask was added compound **5** (1.39 g, 3.81 mmol), bis(pinacolato)diboron (1.26 g, 4.95 mmol), $PdCl_2$(dppf) (0.209 g, 0.286 mmol), potassium acetate (1.12 g, 11.4 mmol), and 1,4-dioxane (20 mL). The reaction was purged with nitrogen and heated at 100 °C for 3 h. After cooling to room temperature, the mixture was diluted with EtOAc, washed with water and brine and dried. Purification by silica gel chromatography (15−40% EtOAc/hexanes) afforded **7** as a white solid (1.24 g, 79% yield). MS (ESI positive ion) m/z: 331.0 (M (boronic acid) + 1). ^{1}H NMR (400 MHz, $CHCl_3$-d): δ ppm 1.36 (s, 12H), 6.86 (br s, 1H), 7.09−7.17 (m, 2H), 7.74−7.82 (m, 2H), 8.30 (d, J = 1.5 Hz, 1H), 8.45 (d, J = 1.5 Hz, 1H).

***N*-(5-(Benzo[*d*]thiazol-6-yl)-2-chloropyridin-3-yl)-4-fluorobenzenesulfonamide (9).** To a microwave vial equipped with a magnetic stir bar was added 6-bromobenzo[d]thiazole (0.100 g, 0.467 mmol), compound **7** (0.212 g, 0.514 mmol), $PdCl_2$(dppf)·CH_2Cl_2 (0.0191 g, 0.0234 mmol), Cs_2CO_3 (0.457 g, 1.40 mmol), THF (3 mL), and water (0.5 mL). The vial was capped and heated by microwave for 10 min at 100 °C. The reaction mixture was diluted with water (10 mL), DCM (10 mL), and satd NaCl (5 mL). The solution was extracted with DCM (3 × 20 mL), and the combined extracts were dried (Na_2SO_4), filtered, and concentrated in vacuo. The crude product was recrystallized from 5:1 DCM/MeOH and Et_2O. The crystallized material was collected by filtration and washed with Et_2O and dried under vacuum to afford **9** as a tan crystalline solid (0.150 g, 77% yield). HRMS calculated for $C_{18}H_{11}ClFN_3O_2S_2$ (M + H) 420.0037, found 420.0028. ^{1}H NMR (400 MHz, DMSO-d_6): δ ppm 7.42 (t, J = 8.8 Hz, 2H), 7.77−7.89 (m, 3H), 8.08 (d, J = 2.2 Hz, 1H), 8.22 (d, J = 8.4 Hz, 1H), 8.55 (d, J = 1.2 Hz, 1H), 8.63 (d, J = 2.2 Hz, 1H), 9.48 (s, 1H), 10.54 (br s, 1H).

***N*-(6-(6-Chloro-5-(4-fluorophenylsulfonamido)pyridin-3-yl)imidazo[1,2-*b*]pyridazin-2-yl)acetamide (10).** To a 250 mL, round-bottomed flask was added *N*-(6-chloroimidazo[1,2-b]pyridazin-2-yl)acetamide (2.50 g, 11.9 mmol),[27−29] compound **7** (5.39 g, 13.1 mmol), DMSO (50 mL), and aq sodium carbonate (26.7 mL, 53.4 mmol, 2 M). The flask was carefully evacuated and backfilled with N_2. To the mixture was added $PdCl_2(PPh_3)_2$ (0.667 g, 0.950 mmol). The flask was carefully evacuated and backfilled with N_2 and then stirred at 90 °C for 3 h. After cooling to room temperature, the mixture was poured into a solution of pH 4.8 buffer (300 mL, 3 M sodium acetate solution pH adjusted to 4.8) and water (300 mL). A precipitate formed, and the solution was allowed to sit overnight and then was filtered. The filtercake was washed with pH 4.8 buffer and water and then was dried by passing air through the filter. The resulting solid was dissolved in DMF (125 mL) and treated with Siliabond-TAAcONa (11.0 g, 5 equiv relative to mmol of Pd catalyst used, loading = 0.43 mmol/gram, Silicycle brand palladium scavenger, Silicycle). The mixture was heated at 50 °C for 19 h. The solution was filtered through Celite (diatomaceous earth), diluted with diethylamine, filtered through a 0.45 um poly(tetrafluoroethylene) syringe filter, and purified by preparative HPLC (Chiralpak ASH (21 mm × 250 mm, 5 μm) column, 25% B, hold for 0.5 min, ramp up to 45% B at 4% B/min and then ramp up to 60% B at 50% B/min; hold for 2 min and reequilibrate for 1.1 min. Total flow was 50 mL/min, outlet pressure was 100 bar, column temperature was 35 °C. A = supercritical CO_2, B = methanol with 0.2% diethylamine). A portion of the purified material (1.20 g) was dissolved in water (100 mL) and treated with AcOH (0.51 mL). A precipitate formed. The solution was stirred for 15 min and then allowed to sit for 2 h. The mixture was filtered, and the filter cake was washed with water (3 × 15 mL) and then dried by letting air pass through the fritted funnel. Further drying under vacuum (250 mtor, 45 °C, 16 h) afforded **10** as a light-brown solid (0.962 g, 18% yield). HRMS calculated for $C_{19}H_{14}ClFN_6O_3S_1$ (M + H) 461.0592, found 461.0578. ^{1}H NMR (400 MHz, DMSO-d_6): δ ppm 2.13 (s, 3H), 7.39−7.48 (m, 2H), 7.80−7.88 (m, 3H), 8.13 (d, J = 9.4 Hz, 1H), 8.31−8.36 (m, 2H), 8.92 (d, J = 2.2 Hz, 1H), 10.57 (s, 1H), 10.96 (s, 1H).

***N*-(5-(2-Aminoimidazo[1,2-*b*]pyridazin-6-yl)-2-chloropyridin-3-yl)-4-fluorobenzenesulfonamide (11).** To a 100 mL, round-bottomed flask was added **10** (150 mg, 0.33 mmol), methanol (10 mL), and NaOH (10 N, 5 mL). The mixture was heated at reflux for 2 h. The solution was cooled to 0 °C, and 10 N HCl was added until pH = 7. The solution was concentrated and purified by silica gel chromatography (10−50% MeOH/CH_2Cl_2). Further purification by preparative HPLC (Phenomenex Synergi 4 μ MAX-RP 150 mm × 21.2 mm, 40−90% CH_3CN/H_2O, 0.1% TFA, over 15 min) (Phenomenex, Torrance, CA) provided **11** as a yellow solid (20 mg, 15% yield). HRMS calculated for $C_{17}H_{12}ClFN_6O_2S_1$ (M + H) 419.0487, found 419.0476. ^{1}H NMR (400 MHz, DMSO-d_6): δ ppm 7.28 (t, J = 8.8 Hz, 1H), 7.22−7.31 (m, 1H), 7.49 (s, 1H), 7.55 (d, J = 9.2 Hz, 1H), 7.70−7.77 (m, 1H), 7.82−7.90 (m, 2H), 8.52 (d, J = 2.2 Hz, 1H), 8.72 (d, J = 2.2 Hz, 1H).

***N*-(2-Chloro-5-(imidazo[1,2-*b*]pyridazin-6-yl)pyridin-3-yl)-4-fluorobenzenesulfonamide (12).** A 15 mL reaction vial was charged with 6-chloroimidazo[1,2-b]pyridazine (60 mg, 391 μmol), compound **7** (193 mg, 469 μmol), dioxane (2 mL), and water (1 mL). The vial was sealed and purged with N_2 for several minutes. Then it was heated at 100 °C for 1 h. After cooling to room temperature, the phases were separated and the organic phase was dried over Na_2SO_4 and concentrated under vacuum. Purification by silica gel chromatography (1−4% MeOH/DCM) afforded **12** as a white solid (73 mg, 46% yield). HRMS calculated for $C_{17}H_{11}ClFN_5O_2S_1$ (M + H) 404.0378, found 404.0370. ^{1}H NMR (400 MHz, DMSO-d_6): δ ppm 7.45 (t, J = 8.8 Hz, 2H), 7.79−7.87 (m, 2H), 7.88 (d, J = 2.9 Hz, 2H), 8.30 (d, J = 9.4 Hz, 1H), 8.39 (d, J = 2.2 Hz, 1H), 8.43 (s, 1H), 8.92 (d, J = 2.0 Hz, 1H), 10.36−10.74 (m, 1H).

***N*-(6-(6-Chloro-5-(4-fluorophenylsulfonamido)pyridin-3-yl)imidazo[1,2-*a*]pyridin-2-yl)acetamide (13).** To a 10 mL round-bottomed flask was added compound **7** (0.14 g, 0.35 mmol), *N*-(6-bromoimidazo[1,2-a]pyridin-2-yl)acetamide (0.080 g, 0.31 mmol),[27−29] DMSO (3.0 mL), and aq Na_2CO_3 (0.94 mL, 1.9 mmol, 2 M). The flask was carefully evacuated and backfilled with N_2. To the mixture was added $PdCl_2(PPh_3)_2$ (0.022 g, 0.031 mmol). The flask was carefully evacuated and backfilled with N_2 again and then stirred at 95 °C for 1 h. After cooling to room temperature, the mixture was poured into a solution of pH 4.8 buffer (25 mL, 3 M sodium acetate pH adjusted to 4.8), and water (25 mL) and filtered. The filter cake was washed with water (2×) and DCM (2×) and then dried under vacuum to afford **13** as a tan solid (0.102 g, 70% yield). HRMS calculated for $C_{20}H_{15}ClFN_5O_3S_1$ (M + H) 460.0639, found 460.06445. ^{1}H NMR (400 MHz, DMSO-d_6): δ ppm 2.08 (s, 3H), 7.16−7.23 (m, 3H), 7.48 (d, J = 9.2 Hz, 1H), 7.65 (d, J = 2.3 Hz, 1H), 7.73 (d, J = 2.2 Hz, 1H), 7.78−7.82 (m, 2H), 8.14 (s, 1H), 8.72 (s, 1H), 10.69 (s, 1H), 11.95 (br s, 1H).

***N*-(5-(2-Aminoimidazo[1,2-*a*]pyridin-6-yl)-2-chloropyridin-3-yl)-4-fluorobenzenesulfonamide (14).** To a 10 mL, round-bottomed flask was added compound **7** (0.150 g, 0.363 mmol), 6-bromoimidazo[1,2-a]pyridin-2-amine (0.0700 g, 0.330 mmol), DMSO (3.0 mL), and aq Na_2CO_3 (0.990 mL, 1.98 mmol, 2 M). The

flask was carefully evacuated and backfilled with N_2. To the mixture was added $PdCl_2(PPh_3)_2$ (0.0232 g, 0.0330 mmol). Again, the flask was carefully evacuated and backfilled with N_2 and stirred at 95 °C for 3 h. After cooling to room temperature, the mixture was poured into pH 4.8 buffer (3 M sodium acetate solution pH adjusted to 4.8) and diluted with water. The solution was filtered, and the filter cake was washed with water and then 50% CH_2Cl_2/hexane. The aqueous washings were extracted with 25% iPrOH/$CHCl_3$, and the extracts were combined with the filter cake. The combined material was concentrated to remove all of the solvent and the residue was dissolved in MeOH/DCM and concentrated onto silica. Purification by silica gel chromatography (2.0−9.0% MeOH/DCM) afforded **14** as a yellow solid (0.0307 g, 22% yield). HRMS calculated for $C_{18}H_{13}ClFN_5O_2S_1$ (M + H) 418.0534, found 418.0525. ^{1}H NMR (400 MHz, DMSO-d_6): δ ppm 7.08 (s, 1H), 7.34 (br s, 3H), 7.38−7.44 (m, 3H), 7.60 (br s, 2H), 7.78−7.84 (m, 3 H), 7.97 (d, J = 2.2 Hz, 1H), 8.49 (d, J = 2.0 Hz, 1H), 8.77 (s, 1H).

***N*-(2-Chloro-5-(imidazo[1,2-*a*]pyridin-6-yl)pyridin-3-yl)-4-fluorobenzenesulfonamide (15).** A 15 mL reaction tube was charged with compound **7** (130 mg, 315 μmol), 6-bromoimidazo[1,2-*a*]pyridine (155 mg, 788 μmol), $Pd(PPh_3)_4$ (18 mg, 16 μmol), aq Na_2CO_3 (0.47 mL, 0.95 mmol, 2 M), and EtOH (2 mL). The reaction mixture was purged with N_2, sealed and heated at 90 °C for 4 h. After cooling to room temperature, the solution was treated with satd $NaHCO_3$ and extracted with DCM (3×). The combined extracts were washed with water and brine and then dried (Na_2SO_4) and concentrated. Purification by silica gel chromatography (1−4% MeOH (2 M in NH_3)/DCM) afforded **15** (40 mg, 32% yield) as an off-white solid. HRMS calculated for $C_{18}H_{12}ClFN_4O_2S_1$ (M + H) 403.0425, found 403.0443. ^{1}H NMR (400 MHz, DMSO-d_6): δ ppm 7.42 (t, J = 8.9 Hz, 2H), 7.57 (d, J = 9.2 Hz, 1H), 7.68 (s, 1H), 7.72 (d, J = 9.6 Hz, 1H), 7.78−7.87 (m, 2H), 8.03 (s, 1H), 8.07 (d, J = 2.0 Hz, 1H), 8.58 (s, 1H), 9.03 (s, 1H), 10.69 (br s, 1H).

***N*-(5-(6-Chloro-5-(4-fluorophenylsulfonamido)pyridin-3-yl)-1*H*-benzo[*d*]imidazol-2-yl)acetamide (16).** *N*-(6-Bromo-1*H*-benzo[*d*]imidazol-2-yl)acetamide. To a 250 mL, round-bottomed flask was added 6-bromo-1*H*-benzo[*d*]imidazol-2-amine (2.00 g, 9.43 mmol), DCM (100 mL), pyridine (1.0 mL, 12 mmol), and acetic anhydride (0.979 mL, 10.4 mmol). The mixture was stirred at 25 °C for 18 h. The solution was concentrated and then diluted with 10% MeOH (2 M in NH_3)/CH_2Cl_2 until homogeneous and then concentrated onto silica. Purification by silica gel chromatography (0.5−5.0% MeOH (2 M in NH_3)/CH_2Cl_2) afforded the title compound as a white solid (0.676 g, 28% yield). MS (ESI, positive ion) m/z: 254 (M (^{79}Br) + 1).

N-(5-(6-Chloro-5-(4-fluorophenylsulfonamido)pyridin-3-yl)-1*H*-benzo[*d*]imidazol-2-yl)acetamide. To a 25 mL round-bottomed flask was added compound **5** (0.150 g, 0.410 mmol), bis(pinacolato)diboron (0.156 g, 0.615 mmol), potassium acetate (0.161 g, 1.64 mmol), and 1,4-dioxane (4.0 mL). The flask was carefully evacuated and backfilled with N_2. To the solution was added $PdCl_2(dppf)\cdot CH_2Cl_2$ (0.030 g, 0.041 mmol). The flask was carefully evacuated and backfilled with N_2 again and stirred at 90 °C for 6 h. The reaction mixture was allowed to cool to room temperature and to the mixture was added DMF (4.0 mL), *N*-(5-bromo-1*H*-benzo[*d*]imidazol-2-yl)acetamide (0.080 g, 0.31 mmol), and aq Na_2CO_3 (0.79 mL, 1.6 mmol, 2 M). The flask was carefully evacuated and backfilled with N_2. To the mixture was added $PdCl_2(PPh_3)_2$ (0.022 g, 0.031 mmol). The flask was carefully evacuated and backfilled with N_2 again and was stirred at 90 °C for 16 h. After cooling to room temperaure, the solution was poured into satd NaCl (100 mL) and extracted with 25% iPrOH/$CHCl_3$ (3 × 75 mL). The combined extracts were dried (Na_2SO_4) and concentrated. The material was dissolved in MeOH/CH_2Cl_2, concentrated onto silica, and purified by silica gel chromatography (0.5−5.0% MeOH (2 M in NH_3)/CH_2Cl_2) to afford **16** as a white solid (0.0217 g, 15% yield). HRMS calculated for $C_{20}H_{15}ClFN_5O_3S_1$ (M + H) 460.0639, found 460.0659. ^{1}H NMR (400 MHz, DMSO-d_6): δ ppm 2.18 (s, 3H), 7.37 (br s, 1H), 7.44 (t, J = 8.8 Hz, 2H), 7.56 (br s, 1H), 7.70 (br s, 1H), 7.83 (dd, J = 8.8, 5.3 Hz, 2H), 7.91 (s, 1H), 8.56 (br s, 1H), 10.44 (br s, 1H), 11.62 (br s, 1H), 12.16 (br s, 1H).

***N*-(5-(2-Amino-1*H*-benzo[*d*]imidazol-6-yl)-2-chloropyridin-3-yl)-4-fluorobenzenesulfonamide (17).** To a resealable vial was added 2-amino-5-bromobenzimidazole (0.170 g, 0.802 mmol), compound **7** (0.430 g, 1.042 mmol), DMF (8.0 mL), and aq Na_2CO_3 (2.00 mL, 4.01 mmol, 2 M). The flask was carefully evacuated and backfilled with N_2. To the mixture was added $PdCl_2(PPh_3)_2$ (0.056 g, 0.080 mmol). The flask was carefully evacuated and backfilled with N_2 again and then stirred at 90 °C for 2 h. After cooling to room temperature, the mixture was poured into aq $NaHCO_3$ (100 mL) and extracted with 25% iPrOH/$CHCl_3$ (3 × 75 mL). The combined extracts were dried (Na_2SO_4) and concentrated in vacuo to a volume of approximately 10 mL. The material was purified by Prep-HPLC (Phenomenex Gemini 5 μm, C18, 100 mm × 30 mm, 5−60% CH_3CN-(0.1% TFA)/H_2O(0.1% TFA) over 20 min then 100% CH_3CN(0.1% TFA) for 3 min at 20 mL/min) with the fractions containing suspected product concentrated to afford **17** (mono-TFA salt) as an off-white solid (0.0607 g, 14% yield). HRMS calculated for $C_{18}H_{13}ClFN_5O_2S_1$ (M + H) 418.0534, found 418.0518. ^{1}H NMR (400 MHz, DMSO-d_6): δ ppm 7.39−7.55 (m, 3H), 7.61 (s, 1H), 7.76−7.85 (m, 2H), 7.98 (d, J = 2.4 Hz, 1H), 8.57 (d, J = 2.4 Hz, 1H), 8.61 (s, 1H), 12.75 (br s, 1H).

***N*-(5-(1*H*-Benzo[*d*]imidazol-5-yl)-2-chloropyridin-3-yl)-4-fluorobenzenesulfonamide (18).** To a resealable vial was added 5-bromo-1*H*-benzo[*d*]imidazole (0.0800 g, 0.41 mmol), compound **7** (0.20 g, 0.49 mmol), DMF (3.0 mL), and aq K_2CO_3 (1.0 mL, 2.0 mmol, 2 M). The flask was carefully evacuated and backfilled with N_2, and $PdCl_2(PPh_3)_2$ (0.028 g, 0.041 mmol) was added. The flask was carefully evacuated and backfilled with N_2 again and heated at 100 °C for 18 h. After cooling to room temperature, the reaction mixture was poured into a solution of pH 7 buffer (3.0 M NaCl and 0.3 M Sodium Citrate) and water. The solution was filtered, and the filtrate was partially concentrated and extracted with 25% iPrOH/$CHCl_3$ (3 × 30 mL). The combined extracts were washed with satd aq NaCl (25 mL) and then dried (Na_2SO_4) and concentrated onto silica. Purification by silica gel chromatography (1−10% MeOH/CH_2Cl_2) afforded **18** as a white solid (0.034 g, 21% yield). HRMS calculated for $C_{18}H_{12}ClFN_4O_2S_1$ (M + H) 403.0425, found 403.0438. ^{1}H NMR (400 MHz, DMSO-d_6): δ ppm 7.40−7.49 (m, 3H), 7.72 (d, J = 8.4 Hz, 1H), 7.79−7.86 (m, 2H), 7.87 (s, 1H), 7.97 (d, J = 2.4 Hz, 1H), 8.33 (s, 1H), 8.60 (d, J = 2.4 Hz, 1H), 11.60 (br s, 1H).

***N*-(6-(6-Chloro-5-(4-fluorophenylsulfonamido)pyridin-3-yl)benzo[*d*]oxazol-2-yl)acetamide (24).** *N*-(Benzo[*d*]oxazol-2-yl)acetamide. To a round bottomed flask was added benzo[*d*]oxazol-2-amine (0.50 g, 3.7 mmol) and DCM (15 mL). Pyridine (0.30 mL, 3.7 mmol), DMAP (0.023 g, 0.19 mmol), and acetic anhydride (0.37 mL, 3.9 mmol) were added to the mixture. After stirring overnight at room temperature, the mixture was diluted with water and extracted with DCM (4 × 30 mL). The combined organic extracts were dried (Na_2SO_4), filtered, and concentrated in vacuo. The crude product was recrystallized from DCM/hexanes to afford the title compound as a light-yellow crystalline solid (0.450 g, 69% yield). MS (ESI, positive ion) m/z: 177.1 (M + 1). ^{1}H NMR (400 MHz, DMSO-d_6): δ ppm 2.23 (s, 3H), 7.23−7.34 (m, 2H), 7.54−7.63 (m, 2H), 11.62 (s, 1H).

N-(6-Bromobenzo[*d*]oxazol-2-yl)acetamide (**22**). To a round-bottomed flask was added 50% acetic acid (8 mL, 4 mmol), followed by *N*-(benzo[*d*]oxazol-2-yl)acetamide (0.800 g, 5 mmol). DCM (5 mL) was added to the mixture, and the mixture was stirred until homogeneous. Bromine (0.5 mL, 9 mmol) was then added slowly while stirring under an inert atmosphere at room temperature. After 1.5 h, the mixture was diluted with DCM (5 mL) and water (5 mL), and then

sodium thiosulfate was added. After stirring for 15 min, the solution was extracted with DCM (3 × 20 mL). The combined extracts were dried (Na_2SO_4), filtered, and concentrated in vacuo. The crude product was recrystallized from DCM/hexanes to afford **22** as an off-white crystalline solid (0.85 g, 73% yield). MS (ESI, positive ion) m/z: 257.0 (M + 1). ^{1}H NMR (400 MHz, DMSO-d_6): δ ppm 2.22 (s, 3H), 7.45−7.54 (m, 2H), 7.94 (s, 1H), 11.73 (s, 1H).

Potassium trifluoroborate salt **23**. To a round-bottomed flask was added compound **22** (0.635 g, 2.49 mmol), bis(pinacolato)diboron (3.16 g, 12.4 mmol), potassium acetate (0.733 g, 7.47 mmol) and 1,4-dioxane (15 mL). Argon was bubbled into the mixture for 10 min, and then $PdCl_2$(dppf)·DCM (1.02 g, 1.24 mmol) was added. The solution was stirred at 100 °C for 2 days. After cooling to room temperature, the reaction mixture was diluted with satd NaCl and extracted with DCM (4 × 50 mL). The combined extracts were dried (Na_2SO_4), filtered, and concentrated. Purification by silica gel chromatography (10−100% EtOAc/hexanes) afforded a tan oil. This material was dissolved in acetonitrile (10 mL), and potassium hydrogen fluoride (0.731 g, 9.4 mmol) was added and the mixture was stirred at room temperature overnight. The solution was then concentrated in vacuo to afford **23** as a light-yellow solid (0.100 g, 14% yield). MS (ESI, positive ion) m/z: 221 (M (boronic acid) + 1). ^{1}H NMR (400 MHz, MeOH-d_4): δ ppm 2.24 (s, 3H), 7.30−7.43 (m, 1H), 7.47 (d, J = 7.8 Hz, 1H), 7.53 (s, 1H).

N-(6-(6-Chloro-5-(4-fluorophenylsulfonamido)pyridin-3-yl)benzo-[*d*]oxazol-2-yl)acetamide (**24**)To a microwave vial was added compound **23** (0.16 g, 0.57 mmol), compound **5** (0.140 g, 0.38 mmol), $PdCl_2$(dppf)·DCM (0.016 g, 0.019 mmol), Cs_2CO_3 (0.37 g, 1.1 mmol), THF (3 mL), and water (0.5 mL). The vial was capped and then stirred and heated by microwave for 10 min at 100 °C. The mixture was diluted with water (10 mL) and satd NaCl (5 mL). The solution was extracted with DCM (4 × 25 mL), and the combined extracts were dried (Na_2SO_4), filtered, and concentrated. Purification by reverse-phase HPLC afforded **24** (TFA salt) as a tan solid (0.019 g, 11% yield). HRMS calculated for $C_{20}H_{14}ClFN_4O_4S_1$ (M + H) 461.0479, found 461.0485. ^{1}H NMR (400 MHz, DMSO-d_6) δ ppm 3.10 (s, 3H), 7.12 (s, 1H), 7.42−7.45 (m, 2H), 7.81−7.85 (m, 3 H), 8.23 (d, J = 7.2 Hz, 1H), 8.44 (s, 1H), 10.40−10.48 (m, 2H), 10.70 (s, 1H), 10.91 (br s, 1H).

***N*-(5-(2-Aminobenzo[*d*]oxazol-6-yl)-2-chloropyridin-3-yl)-4-fluorobenzenesulfonamide (19).** 6-Bromobenzo[*d*]oxazol-2-amine. To a round-bottomed flask was added benzo[*d*]oxazol-2-amine (0.59 g, 4.0 mmol) followed by 50% acetic acid (2 mL, 1 mmol). Bromine (0.11 mL, 2 mmol) was added slowly, and the mixture was stirred for 1.5 h at room temperature. The mixture was diluted with DCM (5 mL) and water (5 mL), and then sodium thiosulfate was added. After stirring for 15 min, the solution was extracted with DCM (3 × 20 mL), and the combined organic extracts were dried (Na_2SO_4), filtered, and concentrated in vacuo. Purification by silica gel chromatography (5−50% EtOAc/DCM) afforded the title compound as a light-yellow solid (0.60 g, 64% yield). MS (ESI, positive ion) m/z: 214.9 (M + 1). ^{1}H NMR (400 MHz, DMSO-d_6): δ ppm 7.07−7.20 (m, 1H), 7.23−7.36 (m, 1H), 7.55 (s, 2H), 7.60 (d, J = 2.0 Hz, 1H).

N-(5-(2-Aminobenzo[*d*]oxazol-6-yl)-2-chloropyridin-3-yl)-4-fluorobenzenesulfonamide (**19**). To a microwave vial was added 6-bromobenzo-[*d*]oxazol-2-amine (0.075 g, 0.35 mmol), Cs_2CO_3 (0.34 g, 1.1 mmol), $PdCl_2$(dppf)·DCM (0.029 g, 0.035 mmol), compound **7** (0.17 g, 0.42 mmol), THF (3 mL), and water (0.2 mL). The vial was capped and then stirred and heated by microwave for 10 min at 100 °C. The mixture was diluted with water and extracted with DCM (4 × 25 mL). The combined extracts were dried (Na_2SO_4), filtered, and concentrated. The crude product was recrystallized from MeOH and then washed with Et_2O to afford **19** as a tan solid (0.030 g, 20% yield). HRMS calculated for $C_{18}H_{12}ClFN_4O_3S_1$ (M + H) 419.0374, found 419.0376. ^{1}H NMR (400 MHz, MeOH-*d*): δ ppm 7.30 (d, J = 8.2 Hz, 1H), 7.36−7.47 (m, 3H), 7.60 (s, 2H), 7.68 (s, 1H), 7.78−7.83 (m, 2H), 7.92 (d, J = 2.4 Hz, 1H), 8.55 (d, J = 1.8 Hz, 1H), 10.44 (br s, 1H).

***N*-(5-(Benzo[*d*]oxazol-6-yl)-2-chloropyridin-3-yl)-4-fluorobenzenesulfonamide (20).** To a microwave vial was added 6-bromobenzo[*d*]oxazole (0.050 g, 0.25 mmol), Cs_2CO_3 (0.25 g, 0.76 mmol), $PdCl_2$(dppf)·DCM (0.037 g, 0.045 mmol), compound **7** (0.10 g, 0.25 mmol), THF (3 mL), and water (0.5 mL). The vial was capped and then stirred and heated by microwave for 10 min at 100 °C. The mixture was diluted with water and extracted with DCM. The combined organic extracts were dried (Na_2SO_4), filtered, and concentrated. The crude product was recrystallized from 5:1 DCM/MeOH and hexanes to afford **20** as a tan solid (0.040 g, 39% yield). HRMS calculated for $C_{18}H_{11}ClFN_3O_3S_1$ (M + H) 404.0265, found 404.0270. ^{1}H NMR (400 MHz, DMSO-d_6): δ ppm 7.44 (t, J = 8.8 Hz, 2H), 7.71 (d, J = 8.0 Hz, 1H), 7.82 (dd, J = 5.5, 8.0 Hz, 2H), 7.95 (d, J = 8.0 Hz, 1H), 8.07 (s, 1H), 8.17 (s, 1H), 8.66 (s, 1H), 8.85 (s, 1H), 10.53 (br s, 1H).

***N*-(5-([1,2,4]Triazolo[4,3-*a*]pyridin-6-yl)-2-chloropyridin-3-yl)-4-fluorobenzenesulfonamide (21).** To a 15 mL resealable vial was added 6-bromo-[1,2,4]triazolo[4,3-*a*]pyridine (60 mg, 303 μmol), compound **7** (150 mg, 364 μmol), $PdCl_2$(dppf)·DCM (17 mg, 23 μmol), Na_2CO_3 (96 mg, 909 μmol), 1,4-dioxane (2 mL), and water (1 mL). The vial was purged with nitrogen for several minutes and sealed. The reaction mixture was then heated at 100 °C for 1 h. After cooling to room temperature, the organic phase was dried (Na_2SO_4) and concentrated. Purification by silica gel chromatography (1−4% MeOH/DCM) afforded **21** as a light-yellow solid (70 mg, 57% yield). HRMS calculated for $C_{17}H_{11}ClFN_5O_2S_1$ (M + H) 404.0378, found 404.0382. ^{1}H NMR (400 MHz, DMSO-d_6): δ ppm 7.43 (t, J = 8.8 Hz, 2H), 7.7 (d, J = 9.8 Hz, 1H), 7.82 (dd, J = 5.1, 8.8 Hz, 2H), 7.93 (d, J = 10.0 Hz, 1H), 8.14 (d, J = 2.2 Hz, 1H), 8.64 (s, 1H), 9.03 (s, 1H), 9.32 (s, 1H), 10.56 (br s, 1H).

***N*-(5-(Benzo[*d*]isothiazol-5-yl)-2-chloropyridin-3-yl)-4-fluorobenzenesulfonamide (27).** 5-(4,4,5,5-Tetramethyl-1,3,2-dioxaborolan-2-yl)benzo[*d*]isothiazole (**26**). To a 250 mL, round-bottomed flask was added bis(pinacolato)diboron (5.6 g, 22 mmol), 5-bromobenzo-[*d*]isothiazole (**25**, 3.63 g, 17 mmol),[30] potassium acetate (2.5 g, 25 mmol), 1,4-dioxane (100 mL), tricyclohexylphosphine (0.68 g, 2.4 mmol), and tris(dibenzylideneacetone)dipalladium (0) (0.93 g, 1.0 mmol). The mixture was stirred at 80 °C overnight. After cooling to room temperature, the solution was concentrated and purified by silica gel chromatography (0−40% EtOAc/hexane) to afford **26** (3.2 g, 72% yield). ^{1}H NMR (400 MHz, $CDCl_3$): δ ppm 1.41 (s, 12H), 7.91−8.02 (m, 2H), 8.58 (s, 1H), 8.95 (s, 1H).

N-(5-(Benzo[*d*]isothiazol-5-yl)-2-chloropyridin-3-yl)-4-fluorobenzenesulfonamide (**27**). To a 5 mL microwave vial was added boronic ester **26** (0.070 g, 0.30 mmol), compound **5** (0.10 g, 0.30 mmol), aq Na_2CO_3 (0.4 mL, 0.8 mmol, 2 M), FibreCat 1029 triphenylphosphine (20 wt %, 15 mg), and 1,4-dioxane (3 mL). The vial was sealed and then stirred and heated by microwave for 20 min at 120 °C. The reaction mixture was diluted with water and extracted with DCM (3 × 10 mL). The combined extracts were washed with water and satd aq NaCl and then dried ($MgSO_4$) and concentrated. Purification by silica gel chromatography (15% acetone/hexane) afforded **27** as a light-yellow solid (60.0 mg, 48%). HRMS calculated for $C_{18}H_{11}ClFN_3O_2S_2$ (M + H) 420.0037, found 420.0042. ^{1}H NMR (300 MHz, $CHCl_3$-*d*) δ ppm 7.03 (br s, 1H), 7.13−7.23 (m, 2H), 7.73 (dd, J = 8.5, 1.8 Hz, 1H), 7.80−7.89 (m, 2H), 8.12 (d, J = 8.5 Hz, 1H), 8.25 (s, 1H), 8.30 (s, 1H), 8.47 (d, J = 2.3 Hz, 1H), 9.04 (s, 1H).

Hepatocyte Incubation Conditions. Compounds (20 μM) were incubated in freshly isolated hepatocytes at 2 million cells/mL in Krebs−Henseleit buffer for 0 h (control) or 2 h at 37 °C in a shaking water bath saturated with 95% oxygen/5% carbon dioxide. Reactions were quenched with an equal volume of acetonitrile containing 0.3% formic acid, vortex-mixed, and centrifuged at 14000 rpm for 10 min.

Supernatants were separated by reverse phase HPLC (Agilent 1100, Delaware, DE) on a C18 column (Waters C18, 2.0 mm × 150 mm, 3 μm) in-line with an ion-trap mass spectrometer (LTQ; Thermo Fisher Inc., San Jose, CA) employing electrospray ionization in positive ion mode.

Akt Phosphorylation in the U87 MG Tumor Xenograft Model: Dose Response and Time Course PD Assay. The effect of compound **10** on Akt phosphorylation was evaluated in the U87 MG glioblastoma tumor model grown in female CD1 NU/NU mice. Mice were implanted subcutaneously with 5×10^6 U87 MG cells. Treatment with compound **10** at 0.3, 1, or 3 mg/kg by oral administration was initiated when tumor size achieved ~300−400 mm^3. Mice were sacrificed at 3, 8, 16, and 24 h after a single dose and tumors were immediately removed and snap frozen. Levels of phosphorylated Akt versus total Akt were determined by a quantitative MSD assay. Akt phosphorylation measured in tumors from mice treated with vehicle served as a negative control and indicated the background level of phosphorylation.

U87 Tumor Xenograft pAkt (S473) MSD Assay Protocol. Each U87 tumor xenograft was homogenized in 1 mL of ice-cold MSD lysis buffer (containing 150 mM NaCl, 20 mM Tris, pH 7.5, 1 mM EDTA, 1 mM EGTA, 1% Triton-X-100, 1/10 protease inhibitor tablet (Roche, catalogue no. 1836170), 20 μL of phosphatase inhibitor I (Sigma-Aldrich, Inc., catalogue no. P-2850), 20 μL of phosphatase inhibitor II (Sigma-Aldrich, Inc., catalogue no. P-5726), and 40 mM NaF) with GenoGrinder 2000 (BT&C Inc., product no. SP2100−115) at 350 strokes per min for 2 min at room temperature. The lysate was centrifuged twice in a 1.5 mL Eppendorf microcentrifuge tube at 14000 rpm for 15 min at 4 °C. The supernatant was precleared with Protein A/G beads (PIERCE, product no. 20421) in an Eppendorf microcentrifuge tube at 4 °C for 1 h. The beads were centrifuged at 14000 rpm for 15 min at 4 °C, and the supernatant was transferred to a clean Eppendorf microcentrifuge tube. The protein concentration of each sample was determined using Bio-Rad DC protein assay (Bio-Rad, catalogue no. 500−0116) and normalized to a final concentration of 1 mg/mL.

The levels of phosphorylated Akt (S473) and total Akt in tumor xenograft lysates were detected using Meso Scale Discovery phospho-Akt (S473) (catalogue no. K151CAD-2) and total Akt (catalogue no. K151CBD-2) whole cell lysate kits: pAkt (S473) MSD plate and total Akt MSD plate were blocked with 150 μL MSD blocking solution (containing 3% bovine serum albumin, 50 mM Tris, pH 7.5, 150 mM NaCl and 0.02% Tween-20) and incubated at room temperature for 1 h. The plates were then washed four times with 300 μL of MSD Tris wash buffer (containing 50 mM Tris, pH 7.5, 150 mM NaCl, and 0.02% Tween-20). Tumor xenograft lysate (25 μL, 1 mg/mL) was dispensed to each well of the MSD plate. The plate was incubated with shaking in an Eppendorf thermomixer R (Eppendorf, product no. 22670107) at 600 rpm at room temperature for 2 h. The plate was then washed four times with 300 μL of MSD Tris wash buffer. Anti-pAkt (S473) or antitotal Akt detection antibody solution (25 μL, 1.5 μg/mL) was added to each well of the MSD plate. The plate was incubated with shaking in an Eppendorf thermomixer R at 600 rpm at room temperature for 1 h. The plate was then washed four times with 300 μL of MSD Tris wash buffer. MSD read buffer (150 μL, 1×) was added to each well of the MSD plate. The intensity of pAkt (S473) or total Akt signal was measured using MSD sector imager 6000.

The raw phosphorylated Akt (S473) values were divided by the ratio of the mean of total Akt in each group in order to adjust the values for phosphorylated Akt (S473) data to account for varying total Akt levels in individual tissue samples. All results were expressed as the mean ± standard error. Statistical analysis was performed by analysis of variance (ANOVA) followed by Bonferroni−Dunn post hoc test.

■ ASSOCIATED CONTENT

Supporting Information. Plasma and tumor concentrations from in vivo PD assay, calculation methods of ED_{50} and AUC at EC_{50} and AMBIT KINOME*scan* selectivity data for compound **10**. This material is available free of charge via the Internet at http://pubs.acs.org.

■ AUTHOR INFORMATION

Corresponding Author

*Phone: 805-447-8006. E-mail: mstec@amgen.com. Address: One Amgen Center Drive, Thousand Oaks, California 91320-1799, United States

■ ACKNOWLEDGMENT

We thank Yihong Zhou and Shuguang Ma for the metabolite profiling studies, Mike Hayashi for the hepatocyte incubations, Paul Andrews for his assistance with the in vitro U87 MG cellular assay, and Paul Schnier for HRMS analyses.

■ ABBREVIATIONS USED

ANOVA, analysis of variance; AUC, area under the curve; dba, dibenzylideneacetone; DCM, dichloromethane; DMAP, 4-dimethylaminopyridine; dppf, 1,1′-bis(diphenylphosphino)ferrocene; EC, effective concentration; ED, effective dose; EGTA, ethylene glycol bis(2-aminoethyl ether)-*N*,*N*,*N*′,*N*′-tetraacetic acid; HPMC, hydroxypropylmethylcellulose; IC, inhibitory concentration; MSD, mesoscale discovery; mTOR, mammalian target of rapamycin; NaHMDS, sodium hexamethyldisilazide (sodium bis(trimethylsilyl)amide); PD, pharmacodynamic; PI3K, phosphoinositide 3-kinase; PIKK, PI3K-related kinases; POC, percentage of control; PTEN, phosphotase and tensin homologue; QD, once daily; SAR, structure−activity relationship; SD, standard deviation; SE, standard error; TFA, trifluoroacetic acid

■ REFERENCES

(1) Vivanco, I.; Sawyers, C. L. The phosphatidylinositol 3-kinase-AKT pathway in human cancer. *Nature Rev. Cancer* **2002**, *2* (7), 489–501.

(2) Engelman, J. A.; Luo, J.; Cantley, L. C. The evolution of phosphatidylinositol 3-kinases as regulators of growth and metabolism. *Nature Rev. Genet.* **2006**, *7* (8), 606–619.

(3) Bader, A. G.; Kang, S.; Zhao, L.; Vogt, P. K. Oncogenic PI3K deregulates transcription and translation. *Nature Rev. Cancer* **2005**, *5* (12), 921–929.

(4) Samuels, Y.; Wang, Z.; Bardelli, A.; Silliman, N.; Ptak, J.; Szabo, S.; Yan, H.; Gazdar, A.; Powell, S. M.; Riggins, G. J.; Willson, J. K. V.; Markowitz, S.; Kinzler, K. W.; Vogelstein, B.; Velculescu, V. E. High frequency of mutations of the PIK3CA gene in human cancers. *Science* **2004**, *304* (5670), 554.

(5) Zhao, L.; Vogt, P. K. Helical domain and kinase domain mutations in p110alpha of phosphatidylinositol 3-kinase induce gain of function by different mechanisms. *Proc. Natl. Acad. Sci. U.S.A.* **2008**, *105* (7), 2652–2657.

(6) Jarvis, L. M. PI3K at the clinical crossroads. *Chem. Eng. News* **2011**, *89* (15), 15–19.

(7) Liu, P.; Cheng, H.; Roberts, T. M.; Zhao, J. J. Targeting the phosphoinositide 3-kinase pathway in cancer. *Nature Rev. Drug Discovery* **2009**, *8* (8), 627–644.

(8) Cleary, J. M.; Shapiro, G. I. Development of phosphoinositide-3 kinase pathway inhibitors for advanced cancer. *Curr. Oncol. Rep.* **2010**, *12* (2), 87–94.

(9) Carnero, A. Novel inhibitors of the PI3K family. *Expert Opin. Invest. Drugs* **2009**, *18* (9), 1265–1277.

(10) Hennessy, B. T.; Smith, D. L.; Ram, P. T.; Lu, Y.; Mills, G. B. Exploiting the PI3K/AKT pathway for cancer drug discovery. *Nature Rev. Drug Discovery* **2005**, *4* (12), 988–1004.

(11) Kong, D.; Yamori, T. Advances in development of phosphatidylinositol 3-kinase inhibitors. *Curr. Med. Chem.* **2009**, *16* (22), 2839–2854.

(12) Wu, P.; Liu, T.; Hu, Y. PI3K inhibitors for cancer therapy: what has been achieved so far? *Curr. Med. Chem.* **2009**, *16* (8), 916–930.

(13) Braccini, L.; Morello, F.; Perino, A.; Hirsch, E. Post-wortmannin era: novel phosphoinositide 3-kinase inhibitors with potential therapeutic applications. *Curr. Enzyme Inhib.* **2009**, *5* (2), 66–86.

(14) D'Angelo, N. D.; Kim, T.-S.; Andrews, K.; Booker, S. K.; Caenepeel, S.; Chen, K.; D'Amico, D.; Freeman, D.; Jiang, J.; Liu, L.; McCarter, J. D.; San Miguel, T.; Mullady, E. L.; Schrag, M.; Subramanian, R.; Tang, J.; Wahl, R. C.; Wang, L.; Whittington, D. A.; Wu, T.; Xi, N.; Xu, Y.; Yakowec, P.; Yang, K.; Zalameda, L. P.; Zhang, N.; Hughes, P.; Norman, M. H. Discovery and optimization of a series of benzothiazole phosphoinositide 3-kinase (PI3K)/mammalian target of rapamycin (mTOR) dual inhibitors. *J. Med. Chem.* **2011**, *54* (6), 1789–1811.

(15) Booker, S.; D'Angelo, N.; D'Amico, D. C.; Kim, T.-S.; Liu, L.; Meagher, K.; Norman, M. H.; Panter, K.; Schenkel, L. B.; Smith, A. L.; Tamayo, N. A.; Whittington, D. A.; Xi, N.; Yang, K. Preparation of 2-aminobenzothiazole derivatives as phosphoinositide 3-kinase (PI3 kinase) modulators. PCT Int. Appl. WO2009/017822, 2009.

(16) Throughout paper, rat refers to Sprague−Dawley rat, dog refers to beagle dog, and monkey refers to cynomolgus monkey.

(17) Nishimura, N.; Siegmund, A.; Liu, L.; Yang, K.; Bryan, M. C.; Andrews, K.; Bo, Y.; Booker, S. K.; Caenepeel, S.; Freeman, D.; Liao, H.; McCarter, J.; Mullady, E. L.; San Miguel, T.; Subramanian, R.; Tamayo, N.; Wang, L.; Whittington, D. A.; Zalameda, L.; Zhang, N.; Hughes, P. E.; Norman, M. H. Phosphoinositide 3-kinase (PI3K)/mammalian target of rapamycin (mTor) dual inhibitors: discovery and structure−activity relationships of a series of quinoline and quinoxaline derivatives. *J. Med. Chem.* **2011**, doi: 10.1021/jm200386s.

(18) Bengtsson, M.; Larsson, J.; Nikitidis, G.; Storm, P.; Bailey, J. P.; Griffen, E. J.; Arnould, J.-C.; Bird, T. G. C. Preparation of 5-heteroaryl thiazoles and their use as phosphoinositide 3-kinase (PI3K) inhibitors. PCT Int. Appl. WO2006/051270, 2006.

(19) Ishiyama, T.; Murata, M.; Miyaura, N. Palladium(0)-catalyzed cross-coupling reaction of alkoxydiboron with haloarenes: a direct procedure for arylboronic esters. *J. Org. Chem.* **1995**, *60* (23), 7508–7510.

(20) Molander, G. A.; Yun, C.-S.; Ribagorda, M.; Biolatto, B. *B*-Alkyl Suzuki−Miyaura cross-coupling reactions with air-stable potassium alkyltrifluoroborates. *J. Org. Chem.* **2003**, *68* (14), 5534–5539.

(21) Fabian, M. A.; Biggs, W. H.; Treiber, D. K.; Atteridge, C. E.; Azimioara, M. D.; Benedetti, M. G.; Carter, T. A.; Ciceri, P.; Edeen, P. T.; Floyd, M.; Ford, J. M.; Galvin, M.; Gerlach, J. L.; Grotzfeld, R. M.; Herrgard, S.; Insko, D. E.; Insko, M. A.; Lai, A. G.; Lelias, J.-M.; Mehta, S. A.; Milanov, Z. V.; Velasco, A. M.; Wodicka, L. M.; Patel, H. K.; Zarrinkar, P. P.; Lockhart, D. J. A small molecule-kinase interaction map for clinical kinase inhibitors. *Nature Biotechnol.* **2005**, *23* (3), 329–336.

(22) A complete listing of the selectivity screen data is provided in the Supporting Information.

(23) All species were optimized with quantum mechanics using Gaussian 03 as neutral species with density functional theory at the B3LYP/631G* level, using the Polarisable Continuum Model for simulating implicit solvation.

(24) Frisch, M. J.; Trucks, G. W.; Schlegel, H. B.; Scuseria, G. E.; Robb, M. A.; Cheeseman, J. R.; Montgomery, J. A.; Vreven, T.; Kudin, K. N.; Burant, J. C.; Millam, J. M.; Iyengar, S. S.; Tomasi, J.; Barone, V.; Mennucci, B.; Cossi, M.; Scalmani, G.; Rega, N.; Petersson, G. A.; Nakatsuji, H.; Hada, M.; Ehara, M.; Toyota, K.; Fukuda, R.; Hasegawa, J.; Ishida, M.; Nakajima, T.; Honda, Y.; Kitao, O.; Nakai, H.; Klene, M.; Li, X.; Knox, J. E.; Hratchian, H. P.; Cross, J. B.; Bakken, V.; Adamo, C.; Jaramillo, J.; Gomperts, R.; Stratmann, R. E.; Yazyev, O.; Austin, A. J.; Cammi, R.; Pomelli, C.; Ochterski, J. W.; Ayala, P. Y.; Morokuma, K.; Voth, G. A.; Salvador, P.; Dannenberg, J. J.; Zakrzewski, V. G.; Dapprich, S.; Daniels, A. D.; Strain, M. C.; Farkas, O.; Malick, D. K.; Rabuck, A. D.; Raghavachari, K.; Foresman, J. B.; Ortiz, J. V.; Cui, Q.; Baboul, A. G.; Clifford, S.; Cioslowski, J.; Stefanov, B. B.; Liu, G.; Liashenko, A.; Piskorz, P.; Komaromi, I.; Martin, R. L.; Fox, D. J.; Keith, T.; Laham, A.; Peng, C. Y.; Nanayakkara, A.; Challacombe, M.; Gill, P. M. W.; Johnson, B.; Chen, W.; Wong, M. W.; Gonzalez, C.; Pople, J. A. *Gaussian 03, Revision D.01*; Gaussian, Inc.: Wallingford, CT, 2004.

(25) A table describing tumor and plasma concentrations at all doses and time points is provided in the Supporting Information.

(26) Calculation methods of ED_{50} and AUC at ED_{50} are described in the Supporting Information.

(27) Ni, Z.-J.; Pecchi, S.; Burger, M.; Han, W.; Smith, A.; Atallah, G.; Bartulis, S.; Frazier, K.; Verhagen, J.; Zhang, Y.; Iwanowicz, E.; Hendrickson, T.; Knapp, M.; Merritt, H.; Voliva, C.; Wiesmann, M.; Legrand, D. M.; Bruce, I.; Dale, J.; Lan, J.; Levine, B.; Costales, A.; Liu, J.; Pick, T.; Menezes, D. PI-3 Kinase inhibitors and methods of their use. PCT Int. Appl. WO2007/095588, 2007.

(28) Booker, S.; Kim, T.-S.; Liao, H.; Liu, L.; Norman, M. H.; Peterson, E. A.; Stec, M.; Tamayo, N. A. Inhibitors of PI3 Kinase. PCT Int. Appl. WO2009/085230, 2009.

(29) Hamdouchi, C.; Sanchez, C.; Ezquerra, J. Chemoselective arylsulfenylation of 2-aminoimidazo[1,2-*a*]pyridines by phenyliodine-(III) bis(trifluoroacetate) (PIFA). *Synthesis* **1998**, *6*, 867–872.

(30) Molino, B. F.; Liu, S.; Berkowitz, B. A.; Guzzo, P. R.; Beck, J. P.; Cohen, M. Aryl- and heteroaryl-substituted tetrahydroisoquinolines and their preparation, pharmaceutical compositions and use thereof to block reuptake of norepinephrine, dopamine, and serotonin for the treatment of neurological and psychological disorders. PCT Int. Appl. WO2006/020049, 2006.